Effect of local masses on radiated sound pressure from an underwater enclosure due to machine noise

Xia Pan, James Forrest, Ian MacGillivray and Stephen Moore

Maritime Division, Defence Science and Technology Group, Victoria, Australia

ABSTRACT
This paper presents the modelling and analysis of local masses and their effect on the radiated sound pressures from an underwater enclosure. The underwater enclosure is modelled as a submerged cylindrical enclosure with ring stiffeners. To simulate the structure-borne and airborne noise transmission, machine noise is characterised by forces applied along the enclosure in three directions and by acoustic sources located inside of the enclosure. An analytical approach is presented where the inertial force of an added mass is modelled by including a mass-induced pressure in the cylindrical shell equations of motion of the enclosure. Thus, an analytical model implementing the approach can have a number of local masses attached to the surface of the enclosure, which gives insight into how the local masses affect the inherent modal amplitudes for given modal forces. These modal amplitudes determine the radiation characteristics of the underwater structure. The influence of mass sizes and locations on the structure is discussed. For benchmark example cases, the analytical results are compared with those from numerical finite element / boundary element models with good agreement.

1 INTRODUCTION

In maritime applications, it is often important to be able to estimate the noise radiated underwater by a vibrating hull structure due to machine noise during its design stage. A submerged cylindrical enclosure is used here as a simple model to demonstrate the acoustic characteristics of underwater vessels. This paper investigates local masses and their effect on the radiated sound pressure from the enclosure due to machine noise.

Analytical methods based on mathematical modelling can give useful insights into several classes of underwater structural acoustics problems, usually with much shorter computation times than numerical alternatives such as fully coupled finite-element (FE) / boundary element (BE) methods. The numerical methods come into their own, for more complicated built-up structures for which analytical solution is unmanageable. James (1985), Junger & Feit (1993) and Skelton & James (1997) described a range of analytical methods applicable to underwater structural acoustics. Forrest (2016) extended previous work (James, 1985) on sound radiation from a cylinder with acoustic excitation, to allow for the cylinder with longitudinal and circumferential stiffeners. Pan *et al*. (2018, 2019) investigated structural and acoustic responses of a cylinder under arbitrary force and acoustic source excitations.

However, cylindrical structures usually incorporate local masses, which are not accounted for in the Forrest (2016), Pan *et a*l. (2018, 2019) or the other models described above. The presence of local masses attached to the surfaces of structures affects structural and acoustic responses. Only limited results on this topic have been published. The effect of local masses on the vibration of panel structures was investigated by Kopmaz & Telli (2002) and Wong (2002), while the effect of local masses on panel radiation characteristics was investigated by Li (2008) and Sharma *et al*. (2013). Zhang *et al*. (2016) analytically studied the effect of local masses on sound radiation from a panel under force excitation. Their results show that adding a point mass could result in shifting the fundamental frequency to lower value and reducing the radiation at the fundamental frequency. In addition, adding a point mass could significantly increase the radiation from high order modes. They found the radiation efficiency of the fundamental frequency was unlikely affected by the mass, while the radiation efficiencies of high order modes could be significantly increased by the mass. Ekimov & Lebedev (1996) experimentally studied local mass influence on sound radiation from a submerged cylindrical shell excited by an external acoustic source in water. They claimed a small local mass (1% of shell mass) could lead to an increase of acoustic power of 10 to 20 dB at some resonances. All these investigations have clearly shown that the modification level of the structural acoustic responses depends greatly on both the location and the size of the attached mass. However, there were no direct comparisons showing how the degree of influence on sound radiation may differ from structural and acoustic excitations.

This current paper describes the extension of the analytical model originally given by James (1985) and modified by Forrest (2016), to include three orthogonal forces and local masses. The influences of mass sizes and locations on the underwater structure due to force and acoustic source excitations are discussed. To validate the current model, some of the modelled results are compared with those from numerical finite element / boundary element models.

2 ANALYTICAL APPROACH

2.1 Shell Dynamics

A representation of the finite cylindrical hull model for calculating far-field pressure developed by James (1985) is shown in Figure 1(a). The cylindrical hull has two rigid end plates (to form a finite cylindrical enclosure) attached to two semi-infinite cylindrical baffles, so that there is no radiated pressure from the end plates. The acoustic excitation is modelled as a monopole to generate airborne noise. Figure 1(b) shows the cross-section of the hull with an interior monopole source. Figure 1(c) shows three forces applied on the hull in three orthogonal directions to generate structure-borne noise.

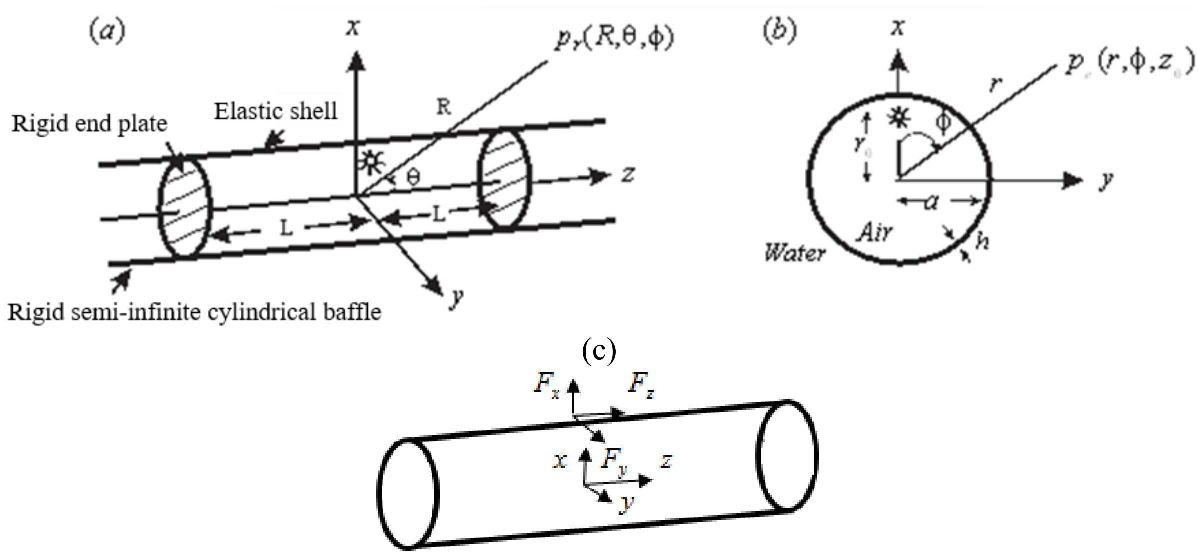

Figure 1: Geometry and coordinate systems of a cylindrical hull: (a) finite cylindrical shell with rigid end plates and a monopole source; (b) cross-section of shell with a monopole source; (c) shell with three orthogonal forces

External loads are represented as surface tractions, i.e. equivalent to pressure or stress, in the equations of motion of the cylindrical shell. To incorporate a local point mass in the model, the inertial force of the mass is therefore modelled by including a mass-induced pressure written in terms of delta functions. The equations of motion for this analysis are based on the Arnold-Warburton formulation (Leissa, 1993) which were modified by Forrest (2016) with added stiffeners on the shell. For a point mass located at (z_c, ϕ_c), the mass-induced pressures in the axial, tangential and radial directions may be written respectively as

$$F_c^a = -\frac{m_c}{a}\delta(\phi-\phi_c)\delta(z-z_c)\ddot{u}(\phi,z), \tag{1a}$$

$$F_c^t = -\frac{m_c}{a}\delta(\phi-\phi_c)\delta(z-z_c)\ddot{v}(\phi,z), \tag{1b}$$

$$F_c^r = -\frac{m_c}{a}\delta(\phi-\phi_c)\delta(z-z_c)\ddot{w}(\phi,z), \tag{1c}$$

where m_c is the mass magnitude, $\delta(\phi,z)$ is the Dirac delta function; $\ddot{u}(\phi,z)$, $\ddot{v}(\phi,z)$ and $\ddot{w}(\phi,z)$ are the accelerations in the axial, tangential and radial directions.

The modal amplitudes of the shell at a particular mode due to structural and acoustic excitations are obtained from the matrix relation:

$$\begin{bmatrix} S_{11} & S_{12} & S_{13} \\ S_{21} & S_{22} & S_{23} \\ S_{31} & S_{32} & S_{33} \end{bmatrix}\begin{bmatrix} U_{mn} \\ V_{mn} \\ W_{mn} \end{bmatrix} = \begin{bmatrix} F_{mn}^a \\ F_{mn}^t \\ F_{mn}^r + F_{mn} \end{bmatrix}. \tag{2}$$

Each element in Equation (2) will be given below. The expressions S_{ij} $(i,j = 1 \text{ to } 3)$, obtained by substituting Equation (1) and three orthogonal displacements into the equations of motion and then taking a Fourier transform, are given by

$$S_{11} = E_1\left[\alpha_m^2 + \frac{(1-\nu)}{2a^2}n^2\right] + K_{As}\alpha_m^2 - \omega^2\left\{\rho_t h + m_c\frac{e_n}{2\pi aL}\left[\cos\frac{m\pi(z_c+L)}{2L}\right]^2[\cos(n\phi_c)]^2\right\},$$

$$S_{12} = E_1\frac{(1-\nu)}{2a^2}\alpha_m n,$$

$$S_{13} = E_1\frac{\nu}{a}\alpha_m - \bar{z}_s K_{As}\alpha_m^3,$$

$$S_{21} = S_{12},$$

$$S_{22} = E_1\left[(1-\nu)\left(\frac{1}{2}+2\beta^2\right)\alpha_m^2 + \frac{1+\beta^2}{a^2}n^2\right] + \frac{K_{Ar}}{a^2}n^2 - \omega^2\left\{\rho_t h + m_c\frac{e_n}{2\pi aL}\left[\sin\frac{m\pi(z_c+L)}{2L}\right]^2[\cos(n\phi_c)]^2\right\},$$

$$S_{23} = E_1\left[\frac{n}{a^2} + \beta^2(2-\nu)\alpha_m^2 n + \frac{\beta^2}{a^2}n^3\right] + \frac{\bar{z}_r K_{Ar}}{a^3}n^3,$$

$$S_{31} = S_{13},$$

$$S_{32} = S_{23},$$

$$S_{33} = E_1\left(\frac{1}{a^2} + \beta^2 a^2\alpha_m^4 + 2\beta^2\alpha_m^2 n^2 + \frac{\beta^2}{a^2}n^4\right) + \frac{K_{Ar}}{a^2} + (K_{Is} + \bar{z}_S^2 K_{As})\alpha_m^4 + \frac{K_{Jr}+K_{Js}}{a^2}\alpha_m^2 n^2$$
$$+ \frac{1}{a^2}\left(K_{Ir} + \frac{\bar{z}_r^2 K_{Ar}}{a^2}\right)n^4 + \frac{2}{a^3}\bar{z}_r K_{Ar} n^2$$
$$-\omega^2\left\{\rho_t h + m_c\frac{e_n}{2\pi aL}\left[\sin\frac{m\pi(z_c+L)}{2L}\right]^2[\cos(n\phi_c)]^2\right\} + \rho_e\omega^2\frac{H_n(\gamma a)}{\gamma H_n'(\gamma a)}. \quad (3)$$

All the symbols in S_{ij} $(i,j = 1 \text{ to } 3)$ are the shell, stiffener and fluid parameters defined in the reference (Forrest, 2016), except for mass parameters in S_{11}, S_{22} and S_{33}. Note S_{11}, S_{22} and S_{33} have been modified to include a local mass magnitude and location. All S_{ij} $(i,j = 1 \text{ to } 3)$ determine modal amplitudes from the modal forces. The modification affects the inherent modal amplitudes for given modal forces. These modal amplitudes determine the three orthogonal displacements and radiated sound pressure, which will be shown below.

In Equation (2), U_{mn}, V_{mn} and W_{mn} are the modal amplitudes in the axial, tangential and radial directions of the shell, m and n are the axial and radial mode numbers, F_{mn}^a, F_{mn}^t and F_{mn}^r are the modal forces due to the axial, tangential and radial force excitation respectively, and F_{mn} is the modal force due to the monopole excitation. The total modal force components due to the axial, tangential and radial forces are given by a sum of the modal components of all the applied forces as

$$\begin{bmatrix} F_{mn}^a \\ F_{mn}^t \\ F_{mn}^r \end{bmatrix} = \frac{e_n F_0}{2\pi aL}\sum_{s=1}^{g}\begin{Bmatrix} \cos\left[\frac{m\pi(z_s+L)}{2L}\right]\cos(n\phi_s) \\ \sin\left[\frac{m\pi(z_s+L)}{2L}\right]\cos(n\phi_s) \\ \sin\left[\frac{m\pi(z_s+L)}{2L}\right]\cos(n\phi_s) \end{Bmatrix}, \quad (4)$$

where F_0, g, z_s and ϕ_s are respectively force amplitude, number of forces and the s^{th} force location; a and L are the radius and half-length of the hull. For a monopole source inside a cylindrical shell, the excitation stress on the shell is given by internal sound pressure. The modal forces F_{mn} due to the monopole source are obtained from the internal sound pressure at the shell surface and given by James (1985). The modal amplitudes U_{mn}, V_{mn} and W_{mn} in Equation (2) can then be solved with S_{ij} $(i,j = 1 \text{ to } 3)$ and modal forces F_{mn}^a, F_{mn}^t, F_{mn}^r and F_{mn} known.

As only radial displacement determines the far-field sound pressure from the shell, only the radial displacement will be presented here. The total radial displacement of the submerged shell due to any radial, axial or tangential force, or an acoustic source, is given by a double Fourier series as

$$W(\phi,z) = \sum_{m=1}^{\infty}\sum_{n=0}^{\infty} W_{mn}\sin\left[\frac{m\pi(z+L)}{2L}\right]\cdot\begin{cases}\cos(n\phi) & \text{for radial/axial force, source} \quad (5a)\\ \sin(n\phi) & \text{for tangential force} \quad (5b)\end{cases},$$

where W_{mn} represents the modal displacements due to the particular force. The overall radial displacement due to a number of forces applied is the superposition of the $W(\phi, z)$ results for each force.

2.2 Far-field Pressure

The pressure radiated from a cylindrical shell to the far-field due to the monopole source is given by James (1985). This pressure is extended to include three orthogonal forces as

$$p_r(R, \theta, \emptyset) = -j\omega\rho_e c_e \frac{e^{jk_e R}}{\pi R} \sum_{m=1}^{\infty} \sum_{n=1}^{\infty} \frac{G_{mn}(\alpha) e^{-\frac{jn\pi}{2}}}{\sin\theta \cdot H_n'(k_e\, a \sin\theta)}, \tag{6}$$

where $\alpha = k_e \cos\theta$ and $G_{mn}(\alpha)$ is the Fourier integral transform of the Fourier series amplitude for the cylinder's radial displacement given by James (1985).

3 NUMERICAL METHODS

For validation of the analytical method, a numerical method using FE/BE software was developed. As the authors had access to and experience with the commercial software Sysnoise, this package was used. Sysnoise is generally able to incorporate heavy fluid loading using a modal analysis and the subsequent computation of heavy-fluid-loaded coupled modes. However, the software is old and is not suited to dealing with fully-coupled problems where two different fluids in interior and exterior domains interact with a structure. Because the interior fluid is of low density compared with the mass of the steel shell it does not significantly affect the vibration of the shell so an attempt was made to use this knowledge to compute the external radiation for the interior air source using the following method.

The numerical FE/BE modelling was performed using a four-stage process. In the first stage the physical structure of the cylinder was built and a FE modal analysis in vacuo with appropriate boundary conditions was performed using the Sysnoise FE structural module. For the second stage, a modal analysis for the cylinder within the external fluid was performed using the uncoupled modes within a fully coupled exterior direct BE calculation within Sysnoise. In the third stage, the acoustic/structural analysis of the interior of the cylinder was performed using the coupled modes from stage two. This approach relies on the negligible effect of the interior air on the exterior-coupled modes so that there is only small 'cross-coupling' between the two fluid regions. The coupled modes of the second stage were expected to be valid for the interior problem as the air-coupled modes for the interior calculation are almost identical with the external fluid-coupled modes of the external calculation. The structural displacements of the cylinder were obtained at this point for an internal sound source using the fully coupled interior direct BE calculation of Sysnoise. In the fourth stage the derived displacements from stage 3 are used as a vibration boundary condition for the exterior problem. In this way the radiated sound for an internal sound source is obtained.

This procedure was found to work when the exterior and interior domains were both air, but did not work well when the exterior domain was water. Hence, Sysnoise comparisons will only be presented for the case where air is also the exterior fluid with acoustic source excitation. This issue can be solved by using a fully coupled FE/BE method such as that described in a separate paper (Pan et al. 2013) or by using more recent fully coupled FE/BE software such as Sysnoise's successor VL-Acoustics or COMSOL multiphysics.

4 RESULTS

4.1 Analytical Results

The underwater enclosure was modelled as a submerged cylindrical enclosure with ring stiffeners and local masses. The analytical calculation is based on a steel hull of 10 m length, 1 m radius and 0.01 m thickness. The ring stiffeners are T-beams, whose spacing is based on 79 ring stiffeners dividing the cylinder length into 80 bays as described by Forrest (2016). Only one local mass varying in magnitude and location is applied on the hull for demonstration. Figure 2 shows excitation locations and different locations of the local mass. Unless indicated, the input force amplitude is 1 N and the source strength of an input monopole is modelled as 1 W sound power in free space. The input force is located halfway along the length of the top of the hull, and the acoustic source is located at 0.67 m above the origin, which is at the centre of the cylinder. Damping in the hull wall is included by using a complex representation of the Young's modulus $E = E(1 - i\eta)$, where η is the loss factor and has a value of 0.02.

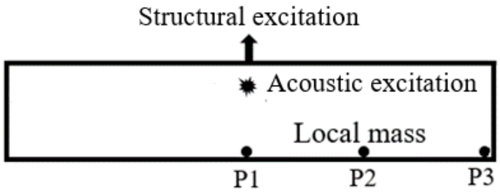

Figure 2: Excitation locations and different locations of the local mass for three separate scenarios examined

In this section, the results of the far-field sound pressure from the plain hull are compared to those with a local mass. Figures 3(a) shows the effect of mass magnitudes on the radiated sound pressure due to the force excitation, observed in the force direction. The mass magnitudes are 15%, 30% and 45% of the plain shell weight. Figure 3(a) indicates due to added mass, the resonant peaks are shifted to lower values in the frequency range. This phenomenon is more pronounced when the mass magnitude increases, as expected. The phenomenon is similar to that reported by Zhang *et al*. (2016), where a mass was attached to a plate and excited by a normal force. Figure 3(b) shows the effect of the mass location. The effect of the mass location is more pronounced as the mass moves towards the halfway location at the bottom hull (P1). This is because the hull has simply supported boundary conditions and there is a constraint in the radial direction at the boundary. Comparing Figures 3(a) with Figure 3(b), the effect of mass magnitudes is more notable than that of mass locations for the current model with the force excitation. Added mass has very little effect on the sound radiation at lower frequency before the resonance-related peaks in radiated sound appear.

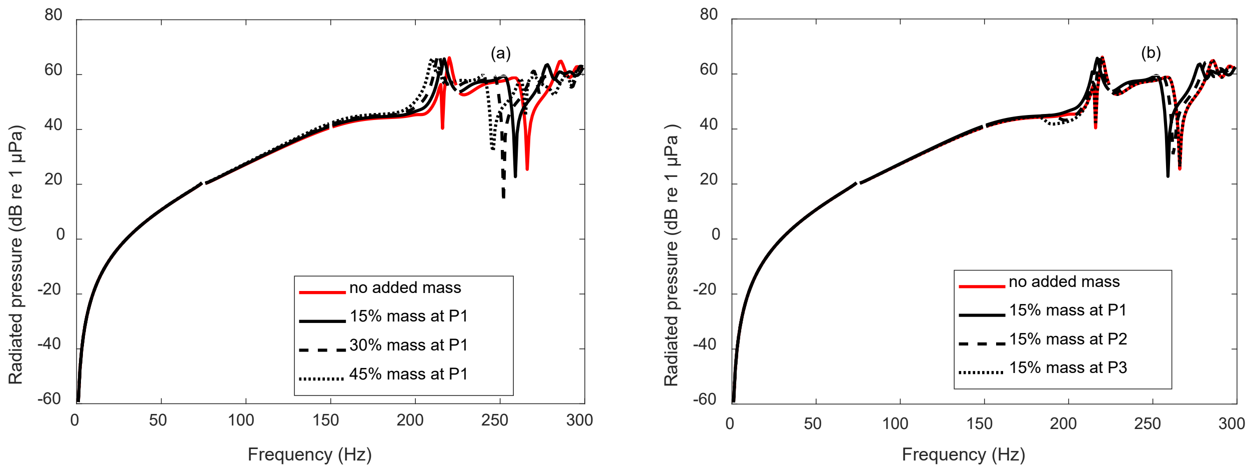

Figure 3: Comparison of far-field sound pressure at 1000 m from the enclosure due to force excitation (pressure at the force direction), without and with a local mass: (a) various magnitudes; (b) various locations

Figures 4(a) and 4(b) show the corresponding results, but the far-field sound pressure is observed perpendicular to the force direction. Comparing Figures 4(a) and 4(b) with Figures 3(a) and 3(b) respectively, the effects of mass magnitudes and locations are slightly different. In particularly, it is observed that the added mass can increase the pressure for some higher order modes, which was also found by Zhang et al. (2016).

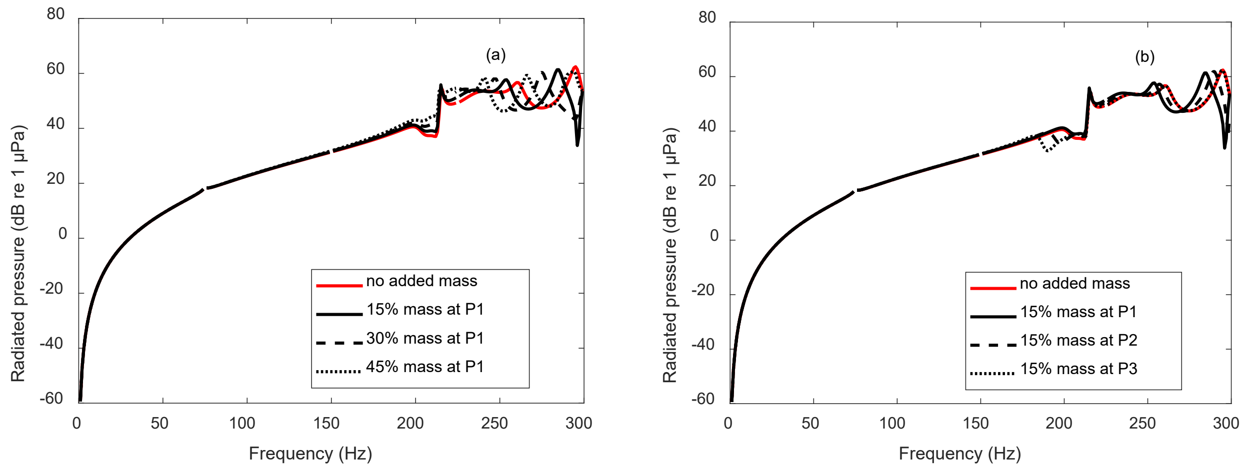

Figure 4: Comparison of far-field sound pressure at 1000 m from the enclosure due to force excitation (pressure perpendicular to force direction), without and with a local mass: (a) various magnitudes; (b) various locations.

Figures 5(a) and 5(b) show the corresponding far-field sound pressures from the hull due to acoustic source excitation, observed directly above the source. It is observed the effects of mass magnitudes and locations on the far-field sound pressure due to the acoustic source excitation are not significant at frequencies below 200 Hz. The modes of the air volume partially determine the radiated noise due to an airborne source, but the lower frequency area is related to one-dimensional modes along the length of the cylinder that do not radiate as effectively through the cylindrical surface. The low frequency modes also have long wavelengths, so their coupling to the cylindrical shell may be less affected by local mass. In addition, an air volume partially determines airborne noise. The current model uses a point mass, so the air volume does not change. At higher frequencies, results shown in Figures 5(a) and 5(b) indicate the added mass can increase significantly the radiated pressure at resonant peaks (see frequencies at 209, 239 and 265 Hz in Figure 5(a)). This phenomenon shows some similarity to that measured by Ekimov & Lebedev (1996), where a submerged cylinder loaded with an external mass was excited by an external acoustic source in the water.

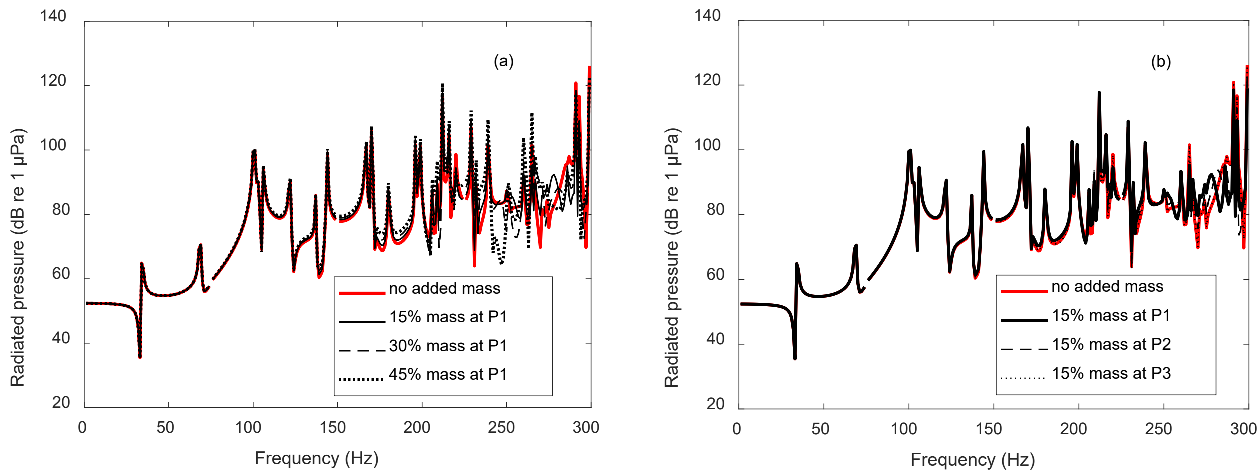

Figure 5: Comparison of far-field sound pressure at 1000 m (above the excitation) from the enclosure due to acoustic source excitation, without and with a local mass: (a) various magnitudes; (b) various locations

4.2 Comparison with Numerical Results

For a benchmark example case, the analytical and numerical results are compared for a plain hull. In this case, a plain steel hull of 2 m length, 1 m radius and 0.01 m thickness with an air-loaded exterior was excited by an internal monopole source located at a distance of 0.67m from the origin along the x-axis (see Figure 1(b)). The source power is equivalent to a 1 W in free space.

Figure 6 compares the internal sound pressure, from the analytical and Sysnoise numerical methods, observed at two radial distances from the origin. Figure 7 presents a comparison of the radiated pressure from the two methods. Results shown in Figures 6 and 7 indicate excellent agreement between the analytical and Sysnoise numerical calculations

.

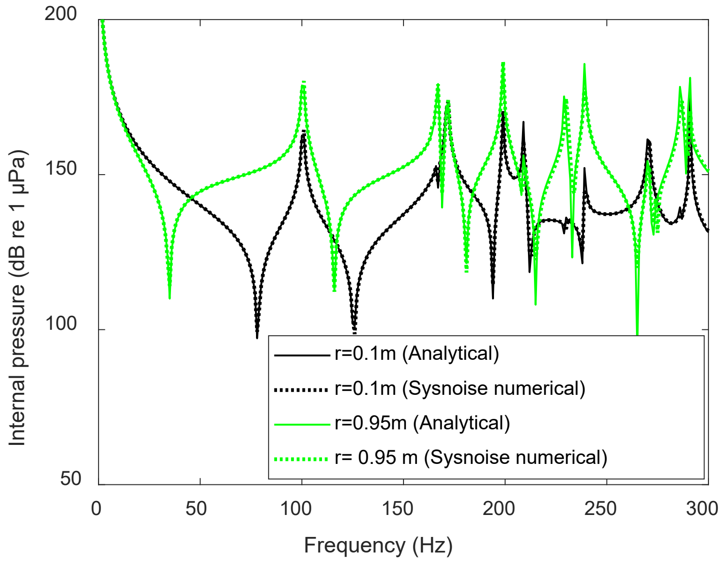

Figure 6: Comparison of analytical internal sound pressures with Sysnoise in an air-loaded plain hull, due to an internal monopole source excitation and the observation point at two distances from the origin

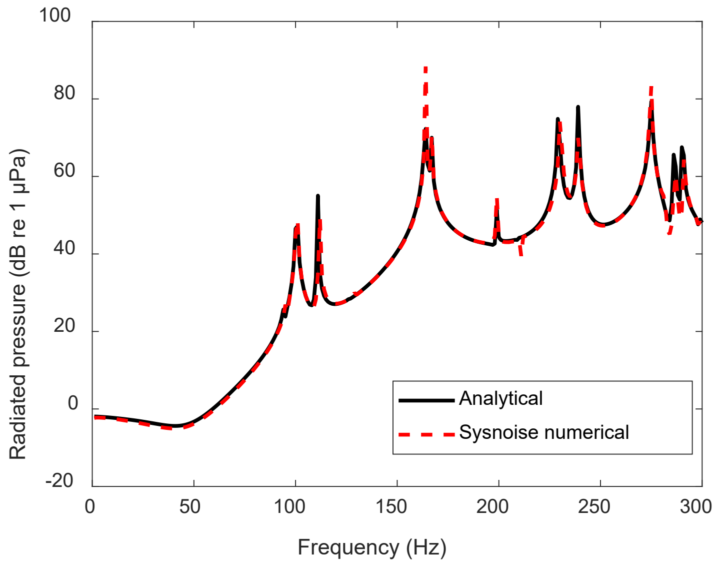

Figure 7: Comparison of analytical far-field sound pressure at 1000 m with Sysnoise from an air-loaded plain hull, due to an internal monopole source excitation

5 CONCLUSIONS

This paper has presented the modelling and analysis of local masses and their effect on radiated sound pressure from an underwater cylindrical enclosure. The enclosure was mathematically modelled to include local point masses and ring stiffeners. The expressions of the radiated sound pressure from the enclosure due to force and acoustic source excitations have been developed. It was found the effect of local masses on the radiated pressure was related to excitations, mass magnitudes, mass locations, and frequency-dependence as described below.

(1) For force excitation, most resonant peaks of the current model were shifted to lower values due to added mass at frequencies between 1 and 300 Hz. This phenomenon was more pronounced when the mass magnitude was increased. The effect of mass locations was related to boundary conditions. It was observed that the added mass could increase the radiated pressure for some higher order modes.

(2) For acoustic source excitation, the effects of mass magnitudes and locations on the radiated pressure were not significant at frequencies below 200 Hz, which may be due to the point-mass limitation. At higher frequencies, the added mass could significantly increase the radiated pressure at resonances.

(3) For a benchmark example case, the analytical results were compared with those from numerical finite element / boundary element models with good agreement.

REFERENCES

Ekimov, A.E. and Lebedev, A.V. (1996). "Experimental study of local mass influence on sound radiation from a thin limited cylindrical shell", *Applied Acoustics*, vol. 48, pp. 47-57. https://doi.org/10.1016/0003-682X(95)00049-F

Forrest, J.A. (2016). "Sound radiation from a submerged stiffened cylinder with acoustic excitation", *Proceedings of Acoustics 2016*, Brisbane, Australia.

James, J.H. (1985). "An approximation to sound radiation from a simply-supported cylindrical shell excited by an interior point source", AMTE(N) TM85024, Admiralty Marine Technology Establishment, Teddington, UK.

Junger, M.C. and Feit, D. (1993). *Sound, Structures and Their Interaction*, Acoustical Society of America, New York.

Kopmaz, O. and Telli, S. (2002). "Free vibrations of a rectangular plate carrying a distributed mass", *Journal of Sound and Vibration*, vol. 251, pp. 39-57. https://doi.org/10.1006/jsvi.2001.3977

Leissa, A. (1993). *Vibration of Shells*, Acoustical Society of America, New York.

Li, S. and Li, X. (2008). "The effects of distributed masses on acoustic radiation behaviour of plates", *Applied Acoustics*, vol. 69, pp. 272-279. https://doi.org/10.1016/j.apacoust.2006.11.004

Pan, X., MacGillivray, I., Tso, Y. and Peters H. (2013). "Investigation of sound radiation from a water-loaded cylindrical enclosure due to airborne noise", *Proceeding of Acoustics 2013*, Victor Harbor, Australia.

Pan, X., MacGillivray, I. and Forrest, J. (2018). "Investigation of structural and acoustic responses of a submerged cylindrical enclosure under arbitrary force excitations", *Proceedings of Acoustics 2018*, Adelaide, Australia.

Pan, X., Wilkes, D. and Forrest, J. (2019). "Investigation of underwater hull radiation due to machine noise", *Proceedings of Acoustics 2019*, Cape Schanck, Victoria, Australia.

Sharma, G., Sarkar, A. and Ganesan, N. (2013). "Acoustic directivity control by point mass attachment", *Proceeding of the 20th International Congress on Sound and Vibration*, Bangkok, Thailand.

Skelton, E.A. and James, J.H. (1997). *Theoretical Acoustics of Underwater Structures*, Imperial College Press, London.

Wong, W.O. (2002). "The effects of distributed mass loading on plate vibration behaviour", *Journal of Sound and Vibration*, vol. 252, pp. 577-583. https://doi.org/10.1006/jsvi.2001.3947

Zhang, P., Wu, H., Ji, L. and Jokić, M. (2016). "A study on the effects of local added masses on the natural and the sound radiation characteristics of thin plate structures", Transactions of FAMENA XL-4 (2016), Zagreb, Croatia. https://doi.org/10.21278/TOF.40403